

The influence of a vegetated bar on channel-bend flow dynamics

Sharon Bywater-Reyes^{1,2}, Rebecca M. Diehl¹, Andrew C. Wilcox¹

¹Department of Geosciences, University of Montana, 32 Campus Drive #1296, Missoula, Montana, 59812-1296, USA

²Department of Earth and Atmospheric Sciences, [University of Northern Colorado](https://www.unco.edu), 501 20 St., Greeley, Colorado, 80639, USA

Correspondence to: Sharon Bywater-Reyes (sharon.bywaterreyes@unco.edu)

The authors declare that they have no conflict of interest.

Abstract. ~~Alternating point bars influence hydraulics, morphodynamics, and channel geometry in alluvial rivers. Recruitment of pioneer woody riparian vegetation is tightly coupled with bar building. Woody riparian vegetation often establishes on point bars and. Once established, vegetation may cause changes in channel-bend hydraulics as a function of vegetation density, morphology, and flow conditions, yet the influence of vegetation on changing bend hydraulics and forces has been unresolved. We used a two-dimensional hydraulic model that accounts for vegetation drag to predict how channel-bend hydraulics are affected by vegetation recruitment on a point bar in a gravel-bed river (Bitterroot River, Montana, United States) to test the sensitivity of channel bend hydraulics to riparian vegetation for a gravel bed river with bars. A The calibrated model for the Bitterroot River, Montana (United States) run for both vegetated and bare earth conditions with and without varied vegetation parameters on a bar shows steep changes in flow hydraulics for vegetated flows compared to bare-bar conditions for flows greater than bankfull up to a 10-year flow (Q_{10}), with limited additional changes thereafter. Vegetation-morphology effects on hydraulics were more pronounced for sparse vegetation compared to dense vegetation. The main effects were 1) reduced flow velocities upstream of the bar; 2) flow steered away from the vegetation patch with up to a 30 % increase in thalweg velocity; and 3) vegetation slows flow upstream of the bar, steers the a shift of the high-velocity core of flow toward the cutbank, and creates a large cross-stream gradient in cross-stream streamwise velocity. These modeled results Results are consistent with a feedback in channels with vegetated bars whereby vegetation on point bars steers flow towards the opposite bank, potentially likely increases bank erosion at the mid- and downstream end of the bend while, and simultaneously increasing rates of bar accretion through reduction in velocity. Collectively, these patterns of morphodynamics influence topographic steering and channel migration rates.~~

1 Introduction

Channel-bend morphodynamics along meandering rivers influence channel morphology, river migration rates, channel-floodplain connectivity, and aquatic habitat. River point bars, fundamental to channel-bend morphology (Blondeaux and

Seminara, 1985; Ikeda et al., 1981), steer flow and induce convective accelerations (Dietrich and Smith, 1983) that influence boundary shear stress (Dietrich and Whiting, 1989) and sediment transport fields (Dietrich and Smith, 1983; Legleiter et al., 2011; Nelson and Smith, 1989). Channel migration rates are furthermore controlled by the collective processes of bar accretion and bank erosion. Bars along the inner bends of river meanders, although typically broadly described as point bars, also
5 comprise chute bars, tail bars, chute bars, and scroll bars that reflect distinct formative conditions (e.g., obstructions and/or stream power variations) and produce distinct morphodynamic feedbacks (Kleinhans and van den Berg, 2011). Erosion of banks and deposition of bars drives the process of channel migration.

Channel ~~bend and bar~~ dynamics can be tightly coupled with the recruitment and succession of riparian vegetation on river bars (Amlin and Rood, 2002; Eke et al., 2014; Karrenberg et al., 2002; Nicholas et al., 2013; Rood et al., 1998). Plants
10 change local hydraulics (Nepf, 2012; Rominger et al., 2010) and sediment transport conditions (Curran and Hession, 2013; Manners et al., 2015; Yager and Schmeeckle, 2013), resulting in strong feedbacks between the recruitment and growth of woody riparian vegetation and bar building (Bendix and Hupp, 2000; Dean and Schmidt, 2011) that can ~~impact~~influence the ~~hydraulics and~~ morphology of rivers at multiple scales (Bywater-Reyes et al., 2017; Osterkamp et al., 2012). Although possible on all bar types, ~~p~~Pioneer vegetation can occur on all bar types but is most~~re~~ likely to survive on nonmigrating bars, such as
15 forced alternating point bars (Wintenberger et al., 2015). Plant traits ~~such as including~~ height, frontal area, and stem flexibility vary with elevation above the baseflow channel, ~~and influence~~ influencing both the susceptibility of plants to uprooting during floods and their impact on morphodynamics ~~effects~~ (Bywater-Reyes et al., 2015, 2017; Diehl et al., 2017a; Kui et al., 2014). Vegetation effects on hydraulics, bank erosion, and channel pattern also depend on the uniformity of vegetation distribution on bars, which can vary depending on wind versus water-based dispersal mechanisms (Van Dijk et al., 2013), and on whether plants occur individually or in patches (Manners et al., 2015).
20

Experimental work in flumes has shown that vegetation is vital to sustaining meandering in coarse-bedded rivers (Braudrick et al., 2009). Vegetation's effect on stabilizing banks, steering flow, and impacting morphodynamics furthermore depends on seed density and stand age. In an experiment, ~~u~~Uniform vegetation on bars has been shown, experimentally, to decrease~~d~~ bank erosion rates, stabilized~~d~~ banks, and increased~~d~~ sinuosity of meander bends (Van Dijk et al., 2013). Gran and
25 Paola (2001) showed that vegetation, by increasing bank strength, generates secondary currents associated with oblique bank impingement that may be more important than helical flows generated by channel curvature. Other ~~F~~ experiments generally suggested vegetated bars decrease velocities over the bar and push flow toward the outer bank. For example, tests in a constructed, meandering laboratory stream with two reed species planted on the ~~a~~ sandy point bar ~~of a constructed, meandering experimental stream~~ showed that and found vegetation reduced velocities ~~y values~~ over the vegetated bar, increased
30 them in the thalweg, strengthened secondary circulation, and directed secondary flow toward the outer bank (Rominger et al., 2010). Another study in the same experimental facility, but using woody seedlings planted on the point bar, also found reduced velocities in the vegetated area of the bar, with the greatest reductions at the upstream end, and the effect varying with vegetation architecture and density (Lightbody et al., 2012). In a flume study where meandering effects were~~was~~ simulated in a straight channel by placing dowels representing vegetation patches in alternating locations along the edges of the flume.

vegetation reduced velocity within and at the edges of the vegetation patch and increased velocities near the opposite bank (Bennett et al., 2002). Experiments in a high-curvature meandering flume, in contrast, showed that vegetation inhibited high shear-stress values from reaching the outer bank (Termini, 2016), inconsistent with studies simulating moderate sinuosity channels.

5

~~In computational modelling of flow and sediment transport, v~~Vegetation's effect on river morphodynamics have also been~~can be~~ simulated with a range of computational models~~approaches~~. Reduced-complexity models that approximate the physics of flow ~~and sediment transport~~ have successfully reproduced many of the features observed in channels influenced by vegetation, such as the development of a single-thread channel (e.g., Murray and Paola, 2003). Two-dimensional models that use shallow-water equations and, in some cases, sediment transport relations, provide an alternative that may be less dependent on initial conditions and more capable of representing the physics of ~~fn~~ vegetation-flow interactions (Boothroyd et al., 2016, 2017; Marjoribanks et al., 2017; Nelson et al., 2016; Nicholas et al., 2013; Pasternack, 2011; Tonina and Jorde, 2013). Investigations of channel-bend dynamics influenced by vegetation using two-dimensional models often represent vegetation by increasing bed roughness (see Green, 2005 and Camporeale et al., 2013 for comprehensive reviews). Nicholas et al. (2013) simulated bar and island evolution in large anabranching rivers using a morphodynamic model of sediment transport, bank erosion, and floodplain development on a multi-century timescale where vegetation was ~~modelled~~modeled using a Chezy roughness coefficient. Asahi et al. (2013) and Eke et al. (2014) ~~modelled~~modeled river bend erosional and depositional processes that included a bank-stability model and deposition dictated by an assumed vegetation encroachment rule. Bertoldi and Siviglia (2014) used a morphodynamic model coupled with a vegetation biomass model, which accounted for species variations in nutrient and water needs to simulate the coevolution of vegetation and bars in gravel-bed rivers. Vegetation was ~~modelled~~modeled as increased bed roughness via the Strickler-Manning relation that varied linearly with biomass. Their model showed two scenarios: one where flooding completely removed vegetation, and one where vegetation survived floods, resulting in vegetated bars. These two alternative stable states (bare versus vegetated bars) have been found experimentally as well (Wang et al., 2016).

25

Although the aforementioned models produce many of the features of river morphodynamic evolution, w~~When~~ vegetation drag is dominant over bed friction, using conventional resistance equations (e.g., Manning's n; roughness) to model vegetation's effect on the flow introduces error. Increasing the roughness within vegetated zones increases the ~~modelled~~modeled shear stress and therefore artificially inflates the sediment transport capacity at the local scale (e.g., vegetation patch or bar), although ~~at the reach reach-scale the~~ results may be appropriate (Baptist et al., 2005; James et al., 2004). An alternative more comparable to flume studies includes ~~Alternative approaches include accounting for v~~Vegetation drag can also be treated in computational models by representing plants explicitly as cylinders (e.g., Baptist et al., 2007; Vargas-Luna et al., 2015a), comparable to the approach of many flume studies, or by accounting for drag from foliage, stems, and streamlining~~streamlined~~ vegetation, but such an approach is currently not widely adopted because of limited ability to specify all parameters, ~~and the altered drag that occurs as a result~~ (e.g., Boothroyd et al., 2015, 2017; Jalonen et al., 2013;

30

Västilä and Järvelä, 2014). Vargas-Luna et al. (2015a) showed through coupling of numerical modeling and experimental work that representing vegetation as cylinders is most appropriate for dense vegetation. Iwasaki et al. (2015) used a two-dimensional model that accounted for vegetation drag to explain morphological change of the Otofuke River, Japan, caused by a large flood event in 2011 that produced substantial channel widening and vegetation-influenced bar building. They found that vegetation allowed bar-induced meandering to maintain moderate sinuosity, whereas in the absence of vegetation, river planform would switch from single-thread to braided. Marjoribanks et al. (2017) modeled the effects of vegetation on channel hydraulics for a small (~5 m wide by 16 m long), straight river reach and found velocity reduced broadly throughout the channel.

As the above review suggests, there have been considerable advances in laboratory and computational modeling of vegetation effects on hydraulics that complement understanding of bar and bend morphodynamics and reciprocal interactions between riparian vegetation and river processes (Corenblit et al., 2007; Gurnell, 2014; Osterkamp and Hupp, 2010; Schnauder and Moggridge, 2009). Challenges persist, however, in representing field-scale complexities in a modeling framework that allows for testing field-scale interactions between plants, flow, and channel morphology on vegetated point bars. Here we tackle key elements of this problem by investigating how the distribution of woody vegetation on a point bar influences bend hydraulics and flow steering across a range of flood magnitudes using a two-dimensional modeling approach informed by high-resolution topography and vegetation morphology data that spatially defines vegetation drag. We model a range of vegetation densities and plant morphologies representing different stages of pioneer woody vegetation growth on a ~~single channel-point~~ bar. We vary discharge in the model to represent the stage-dependent effects of vegetation on hydraulics, as well as different flood stages that may be important for the recruitment of plants and the erosion or deposition of sediment within the channel bend. We predict that the presence of woody vegetation affects bar and meander dynamics by steering flow, thereby influencing the morphodynamic evolution of vegetated channels. Our objectives are to 1)- Determine which vegetation morphology and flow conditions result in the greatest changes to channel-bend hydraulics; and 2)- Infer how these changes in hydraulics would impact channel-bend morphodynamics and evolution. The insights derived from our ~~analyses-analysis~~ are relevant ~~to-for~~ understanding ecogeomorphic feedbacks ~~between riparian ecosystems and physical processes~~ in meandering rivers, ~~to~~-understanding how such feedbacks are mediated by plant traits and flow conditions, and ~~to managing for different for~~ riparian plant species management along river corridors.

2 Methods

2.1 Study area

To meet our objectives, we model a point bar-bend sequence on the Bitterroot River, southwest Montana, United States (Fig. 1). Our field site has a pool-riffle morphology and a wandering pattern, with channel bends, ~~alternate-point~~ bars, and woody vegetation on bars and floodplains. The study reach is located on a private reserve (MPG Ranch) with minimal disturbance to the channel and floodplain, and flow and sediment supply are relatively unaltered by flow regulation, because the only

significant dam in the contributing watershed is ~120 km upstream of the study reach, on a tributary, ~~relatively unregulated because few upstream dams are present.~~ Annual mean discharge is $68 \text{ m}^3 \text{ s}^{-1}$, bankfull Shields number is ~~0.0403~~, and median grain size is 23 mm, ~~and drainage area of ~6,200 km².~~ Woody bar vegetation is composed of sand bar willow (*Salix exigua*), and cottonwood (*Populus trichocarpa*) seedlings, saplings, and young trees (Fig. 2a, 2c). Ponderosa pine (*Pinus ponderosa*), gray alder (*Alnus incana*), and black cottonwood (*Populus trichocarpa*) comprise mature floodplain forest species.

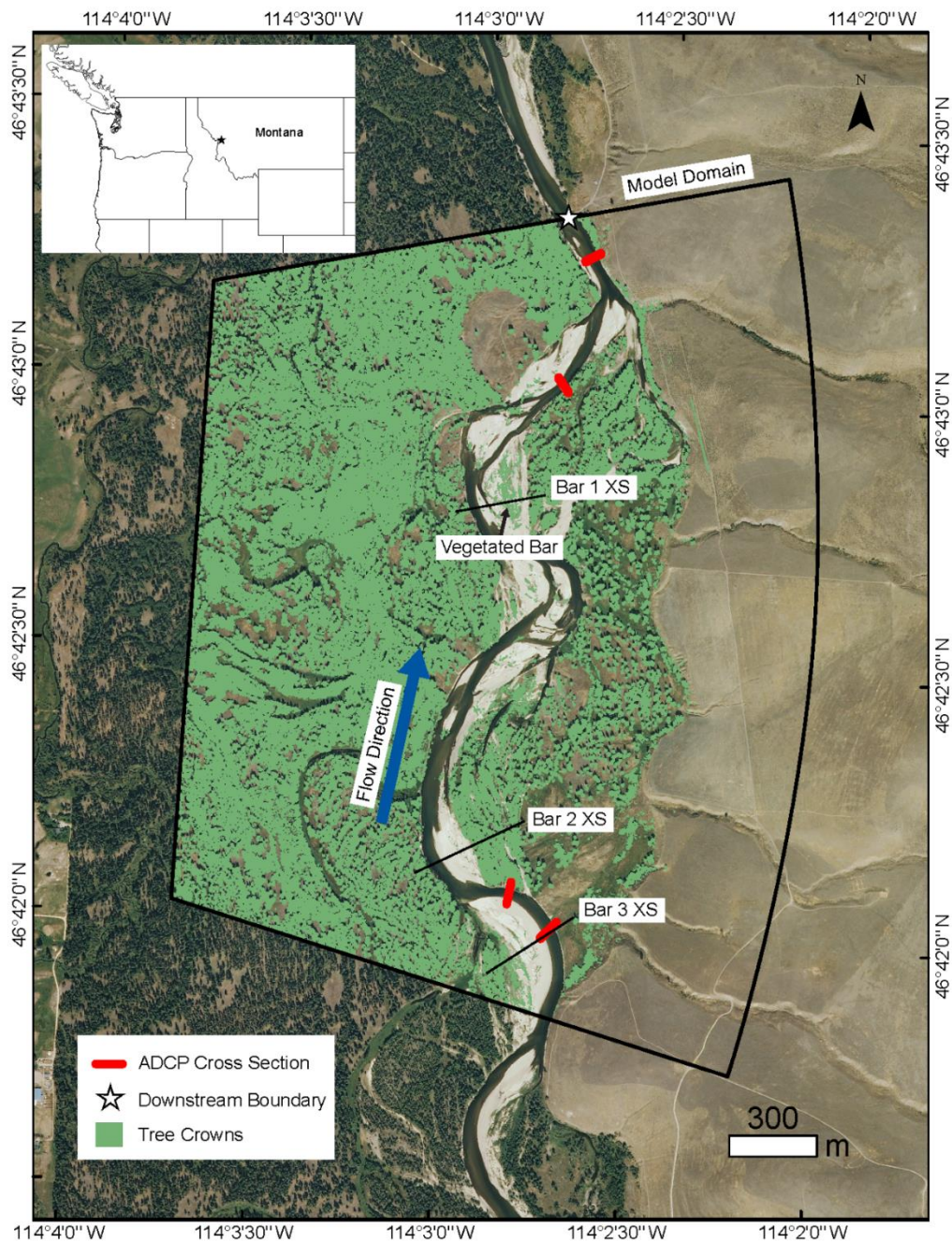
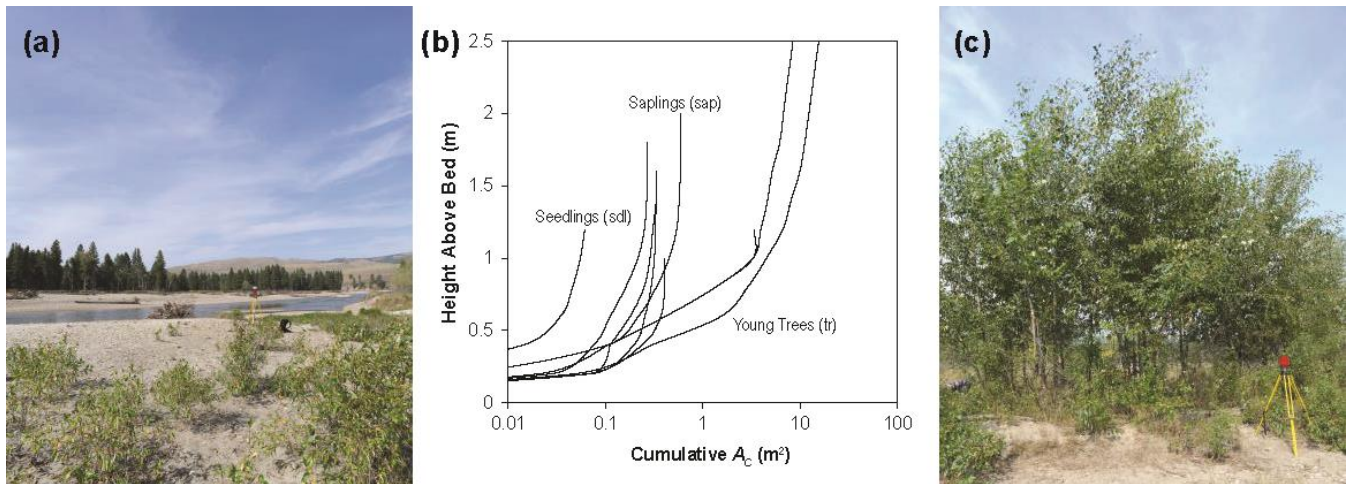


Figure 1. Bitterroot River, Montana showing model domain, ~~showing~~ location of ADCP velocity measurement cross sections, downstream boundary, tree crowns mapped from airborne LiDAR, and the location of the vegetated bar, ~~and the three bars shown in Fig. 9.~~



5 **Figure 2. Modelled/Modeled vegetated bar (a) on the Bitterroot River, showing sparse *Populus* seedlings and saplings. Cumulative A_c (projected vertical frontal area) of *Populus* varies with height above the bed, and the age and size of the individual (b); the greatest cumulative A_c is reached for young trees (c). The average A_c profile for seedlings (sdl), saplings (sap), and young trees (tr) was used to assign an A_r-A_c value based on flow depth for each run. Photo credit: Sarah Doelger.**

2.2 Flow model

To characterize the influence of a vegetated bar on channel-bend hydraulics, we used [an edited version of FaSTMECH](#) (version 2.3.2), a hydrostatic, quasi-steady flow model contained within iRIC (Nelson et al., 2016; <http://i-ric.org/en/index.html>). FaSTMECH solves the depth- and Reynolds-averaged momentum equations in the streamwise- (s) and cross-stream- (n) directions, in a channel-fitted curvilinear coordinate system, using a finite-difference solution (Nelson et al., 2003, 2016). [By convention, values of \$u\$ and \$v\$ are positive downstream and toward the left bank, respectively.](#) Bed stress closure is achieved through a drag coefficient (C_d) scheme (C_d), where boundary shear stress (τ) in the streamwise- (s) and stream-normal- (n) directions are estimated as:

$$\tau_s = \rho C_d u \sqrt{(u^2 + v^2)} \quad (1)$$

10 $\tau_n = \rho C_d v \sqrt{(u^2 + v^2)} \quad (2)$ [Details of the modeling process, beyond those provided in the text here, can be found in the Supplement. By convention, values of \$u\$ and \$\tau_s\$ are positive downstream, and \$v\$ and \$\tau_n\$ positive toward the left bank.](#)

We created the flow model domain in FaSTMECH by characterizing the topography and flow boundary conditions (discharge and water surface elevation at the downstream boundary) of a study reach on the Bitterroot River, Montana (Fig. 1). [Topography was surveyed with a combination of airborne LiDAR and RTK-GPS. We surveyed channel topography with a combination of airborne LiDAR, echosounder and RTK GPS surveys \(see Supplement\). The resulting curvilinear orthogonal grid we created had an average cell size of 2.5 by 2.5 m for calibration runs \(described below\), and 5 by 5 m for the remaining runs. \(Trimble R7 and 5800 with Trimble 5700 base station\) \(see Supplement for more detail\). To develop a stage-discharge relationship, we](#) We linked transducer stage measurements at the downstream end of the study reach to discharge derived from USGS 12344000 Bitterroot River near Darby MT, corrected by contributing area for our field site. [Water surface elevations at the downstream boundary for modeled discharges were extracted from the stage-discharge relationship.](#) Discharge was measured at the field site and compared to the adjusted USGS 12344000 value and found to agree within 10 % (Table 1).

Table 1. Calibration flows, showing the channel drag (C_d) and lateral eddy viscosity (LEV), and the root mean square error (RMSE), water surface elevation (WSE), and depth-averaged velocity (\bar{U}).

Run	Discharge ^a ($\text{m}^3 \text{ s}^{-1}$)	C_d	LEV	RMSE- WSE ^b (m)
<u>1</u>	48	0.003	0.04	0.11
	62	0.003	0.004	0.11
<u>2</u>	62 ^{c,d}	0.003	0.04	0.11
	62	0.003	0.4	0.13
<u>3</u>	90	0.003	0.04	0.17
<u>4</u>	453 ^d 453 ^e	0.003	0.04	0.16
<u>5</u>	453 ^d 453 ^{e,f}	0.003	0.04	0.18

25 ^aCorrected by contributing area from USGS 12344000

^bMore details on WSE in Supplement

^bLaw-of-the-wall derived \bar{U} had RMSE 0.24 m s⁻¹; mean measured \bar{U} 1.21 m s⁻¹; mean modeled \bar{U} 1.05 m s⁻¹ (15% error); see Supplement for more details

5 ^cDischarge-^dDischarge measured at site was within 10% of contributing-area-corrected discharge

^dQ₂-^eQ₂ flow

^fVegetation model turned on

10 FaSTMECH uses relaxation coefficients to control changes in a parameter between iterations (Nelson, 2013). Relaxation coefficients were set to 0.5, 0.3, and 0.1 for ERelax, URelax, and ARelax, respectively, through trial and error. Convergence was found after 5000 iterations (mean error discharge < 2 %), considered indicative of adequate model performance for FaSTMECH (Nelson, 2013). We calibrated channel characteristics (bed roughness specified as C_d and lateral eddy viscosity, LEV) and considered them fixed after calibration (Table 1). We used a constant C_d , an approach that has been
15 shown elsewhere to perform comparably to variable roughness in FaSTMECH (e.g., Segura and Pitlick, 2015). We set C_d to minimize the root mean square error (RMSE) of ~~modelled~~modeled water surface elevation (WSE) versus WSE measured in the field from 2011–2015, over a range of calibration flows (see Supplement). ~~We surveyed WSE in locations a.~~ In ~~T~~this calibration process we manually varied C_d values from 0.01 to 0.001, resulting in a C_d of 0.003 and lowest RMSE's for WSE from 0.11 to 0.18-16 m for the lowest and highest calibration flows, respectively (Table 1). Similarly, we manually varied LEV from 0.01 to 0.001 during model calibration, resulting in a LEV value of 0.04, which ~~that~~ minimized RMSE of depth-averaged velocity (\bar{U} =0.24 m s⁻¹; Table 1) between ~~modelled~~modeled values and those measured at four cross sections (Fig. 1; ~~see Supplement for more detail~~) (see Supplement for ~~more~~ details). The RMSE ranges obtained through calibration are consistent with values reported in other studies that have used FaSTMECH (e.g., Legleiter et al., 2011; Mueller and Pitlick, 2014; Segura and Pitlick, 2015), providing confidence in model performance.

25 ~~Relaxation coefficients were set to 0.5, 0.3, and 0.1 for ERelax, URelax, and ARelax, respectively, through trial and error. Convergence was found after 5000 iterations (mean error discharge < 2 %).~~ To address the stage-dependent nature of the impact of a vegetated bar in altering bend hydraulics, we ~~modelled~~modeled flows with magnitudes corresponding to flows with return periods of 2 (Q₂; 453 m³ s⁻¹), 10 (Q₁₀; 650 m³ s⁻¹), 20 (Q₂₀; 715 m³ s⁻¹) and 100 (Q₁₀₀; 800 m³ s⁻¹) years. ~~Because we were unable to maintain a curvilinear, channel fitted grid (nodes overlapped) but were interested in quantifying hydraulics with respect to a channel bend where such a grid is more appropriate, we converted Cartesian coordinate velocity (U_x , U_y) to streamwise and stream-normal values (Fig. 3; Supplement).~~

30

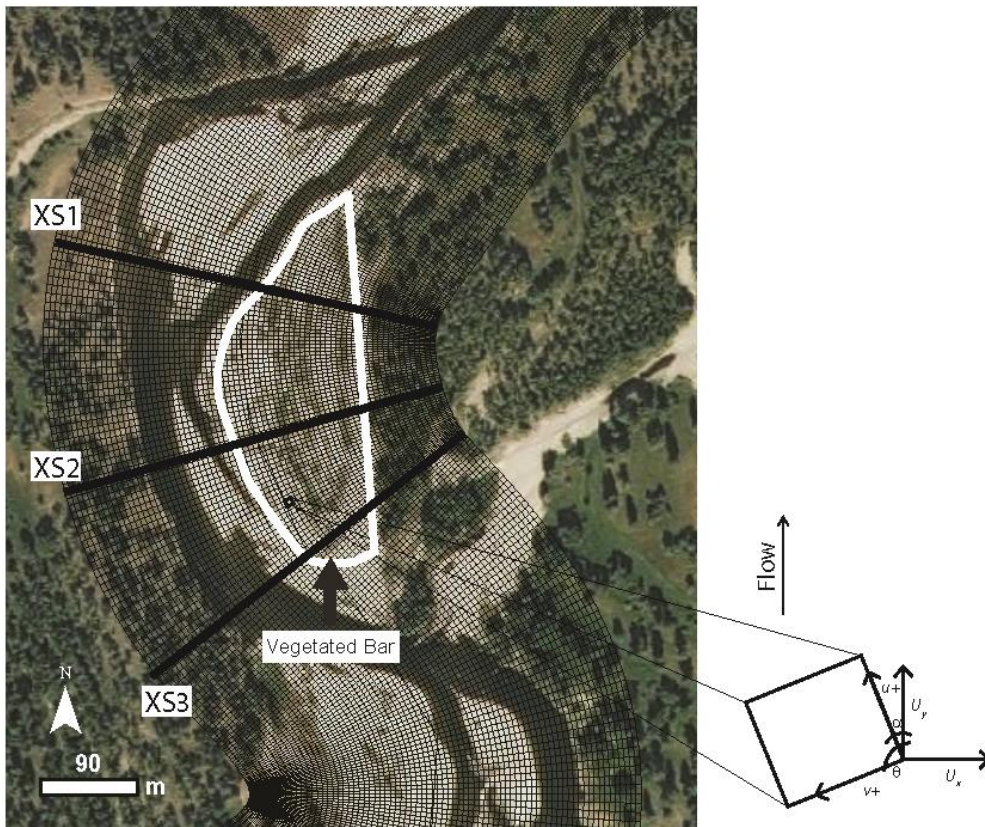


Figure 3. Region around the vegetated bar, showing cross section (XS) locations and the conventions of the curvilinear grid to which model output was converted.

5 **2.3 Modelling** Modeling vegetation's impact on channel-bend hydraulics

We edited FaSTMECH we to accounted for vegetation form drag (F_D) using the following drag equation for rigid vegetation:

$$F_D = \frac{1}{2} \rho C_{d,v} A_c U_c^2 \quad (13)$$

where $C_{d,v}$ is vegetation drag coefficient, A_c is projected vertical frontal area of vegetation (Nepf, 1999; Vargas-Luna et al., 2015, 2016), and U_c is the approach velocity. Drag (F_D) is calculated per bed area (distributed over vegetation polygons).

10 For U_c we substituted used cross-sectional mean node velocity, U_m (after Jalonen et al., 2013). The vegetation drag coefficient ($C_{d,v}$) was assigned a value of one, a first-order approximation also used by others (Boothroyd et al., 2016; Nepf et al., 2013; Vargas-Luna et al., 2016). We modelled modeled vegetation as cylinders by assuming the cylindrical stem frontal area is equal to A_c , specifying vegetation parameters by polygon with an associated stem density (#stems m^{-2}) and height (m; allows for

partitioning of A_c by flow depth). The model assumes a logarithmic velocity profile, although we recognize this is an oversimplification of how factors such as vegetation submergence alter velocity profiles (e.g., Manners et al., 2015).

We focused our analyses on a point bar (Fig. 1) that supports woody riparian vegetation (*Populus* seedlings, saplings, and young trees) most likely recruited mainly by flood dispersal. In our model simulations, we varied vegetation density (#stems m^{-2}) and A_c (m^2 per plant) on the vegetated bar for each of the four flows, and we compared model output to a no-vegetation (no veg) scenario. We considered two vegetation density cases: sparse (*sps*) and dense (*dns*). Our sparse case was based on the average density (0.02 stems m^{-2}) obtained from the airborne LiDAR (see Supplement for more detail). Our dense case (20 stems m^{-2}) was based on the average from random vegetation density plots measured on the bar, which ranged from <1 stem m^{-2} to 227 stems m^{-2} and is consistent with other dense field-measured values (Boyd et al., 2015; van Oorschot et al., 2016; Wilcox and Shafroth, 2013). For A_c , we used ground-based LiDAR to capture vegetation structure (Antonarakis et al., 2010; Bywater-Reyes et al., 2017; Manners et al., 2013; Straatsma et al., 2008). We scanned *Populus* patches representing different stages of pioneer woody vegetation growth: seedlings (*sdl*), saplings (*sap*), and young trees (*tr*). From these scans (postprocessed in the same manner described in (Bywater-Reyes et al., 2017)), we established an A_c –height relationship (Fig. 2b), from which depth-dependent A_c was extracted for each model run by assigning A_c based on the average bar flow depth from the corresponding no-vegetation scenario.

To test whether overbank (floodplain) vegetation (i.e., beyond the vegetated bar) contributes to flow steering in the main channel and influences the hydraulics of the cutbank–bar region of interest (Fig. 3), we included runs with and without floodplain vegetation for each of the four flows and seven bar vegetation scenarios, resulting in 56 model runs. We represented floodplain vegetation as was observed from airborne LiDAR (see Supplement for ~~more~~ detail). These analyses showed that the hydraulics of the cutbank–bar region of interest (Fig. 3) were insensitive to whether or not floodplain vegetation (i.e., beyond the vegetated bar) was present across the range of ~~modelled~~ modeled flow conditions. Therefore the descriptions of hydraulics we present in Results are based only on scenarios varying bar vegetation conditions.

We considered hydraulic ($u, v, \tau_s, \tau_{\#}$) solutions for three cross sections at locations across the bar and cutbank of the channel bend, representing the upstream, midstream, and downstream portion of the bar (Fig. 3). We additionally considered the hydraulics and potential for bed mobility spatially, where the Shields number, τ^* , was used as an indicator of bed mobility:

$$\tau^* = \frac{\tau}{(\rho_s - \rho)gD} \quad (42)$$

where τ is boundary shear stress, ρ_s is sediment density, g is acceleration due to gravity and D is grain diameter. We used the median grain diameter from pebble counts collected on the study bar and along cross sections (Fig. 1). We compared the solutions for vegetation runs for each flow to no-vegetation scenarios to evaluate which configurations had the greatest influence on hydraulics.

3 Results

The effects of point bar vegetation on modelled hydraulics across our study reach are presented here in several ways. First we compare vegetation results, for different density and growth stages, to the no-vegetation case; ~~to vegetated cases (density and growth stages)~~ and second, we compare, ~~and with respect to variations~~ results spatially across ~~the~~ different cross sections across the bar at different discharges. For the no-vegetation case, velocity and shear stress were generally highest in the thalweg and lower over the bar (Fig. 4). Downstream velocity (u) was generally greater than cross-stream velocity (v). The greatest v magnitudes were for the downstream cross section (XS1; Fig. 5c,d). With increasing flow magnitude, both u (Fig. 5b) and v (Fig. 5d) decreased within the thalweg region, but stayed relatively constant over the bar. A similar trend was seen at the mid-bar cross section (XS2) with u decreasing within the thalweg region as flow magnitude increased, but remaining relatively constant over the bar (Fig. 6). In contrast, u increased within the thalweg region and over the bar with increasing flow (Fig. 7a,b) at the upstream cross section (XS3), whereas v stayed relatively constant (Fig. 7c,d).

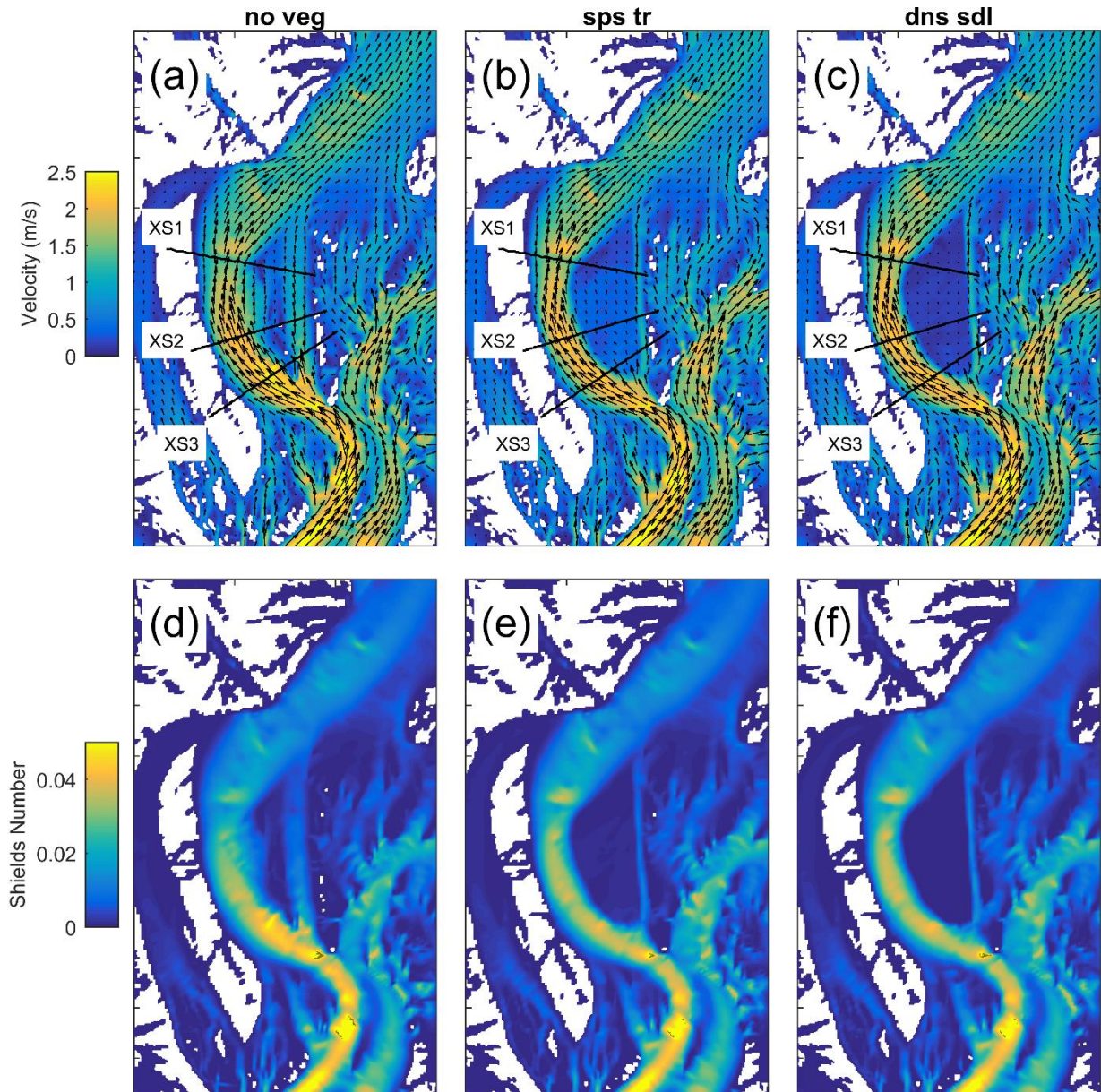


Figure 4. Planview comparison of channel-bend hydraulics (velocity; a–c, and Shields number; c–f) for the Q_{10} no-vegetation (a,d), sparse young trees b,e), and dense seedlings (c,f) runs. Location of cross sections (Fig. 3 shown). Velocity and Shields number are reduced on the bar with increasing size or density of plants, and flow paths within the thalweg and adjacent to the vegetation patch become more concentrated.

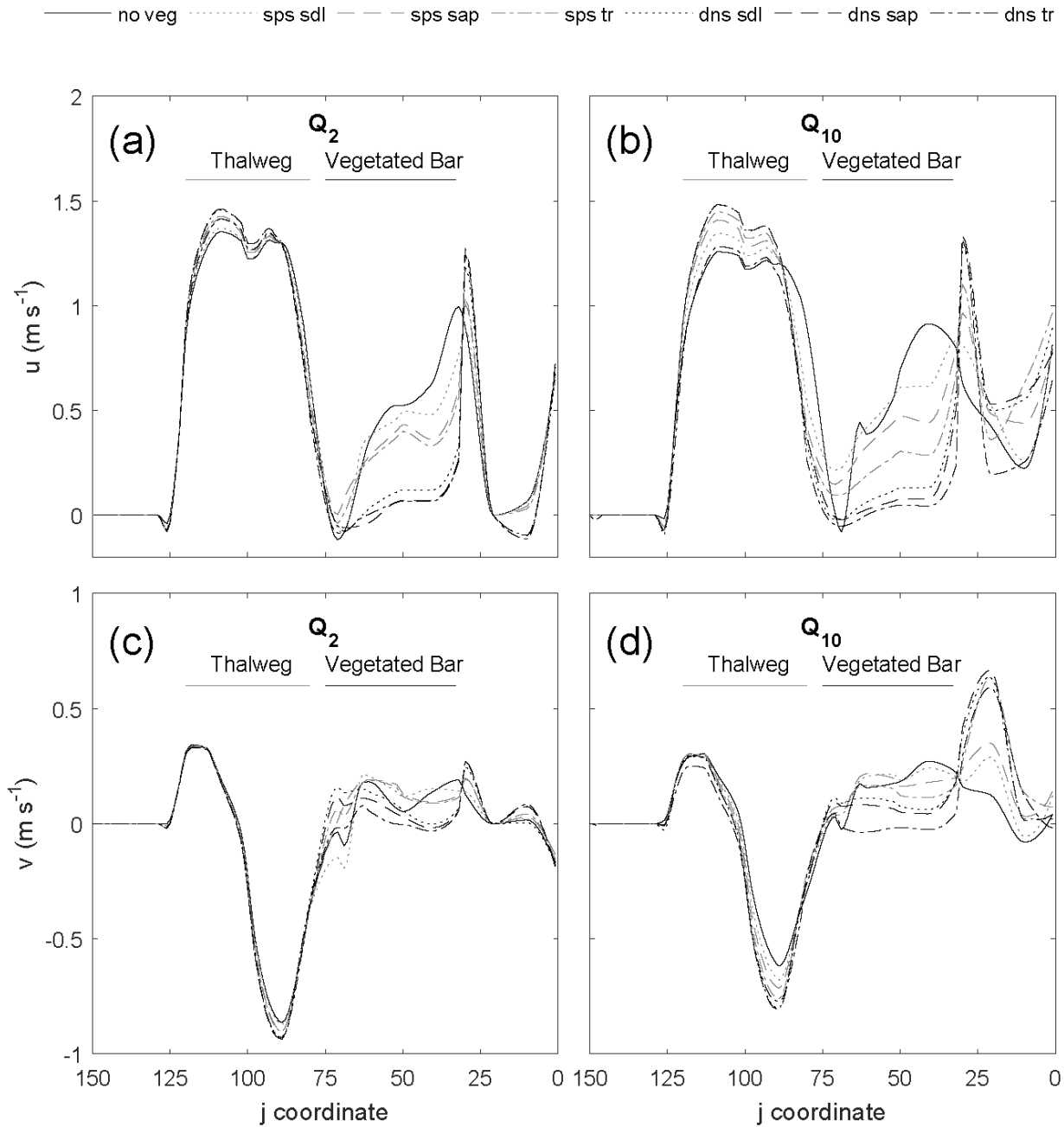


Figure 5. Effect of the vegetated bar ($j = 33\text{--}75$) on the streamwise (u ; a,b) and stream-normal (v ; c,d) velocity at the downstream cross section (XS1) for the Q_2 (a,c) and Q_{10} (b,d) flows. With increasing discharge, plant size (seedling to young trees) and density, u is increased and v decreased within the thalweg ($j = 100$). Both u and v (positive downstream and toward left bank, respectively) are decreased over the bar, and for the sparse young trees and all dense scenarios increased at the edge of the patch.

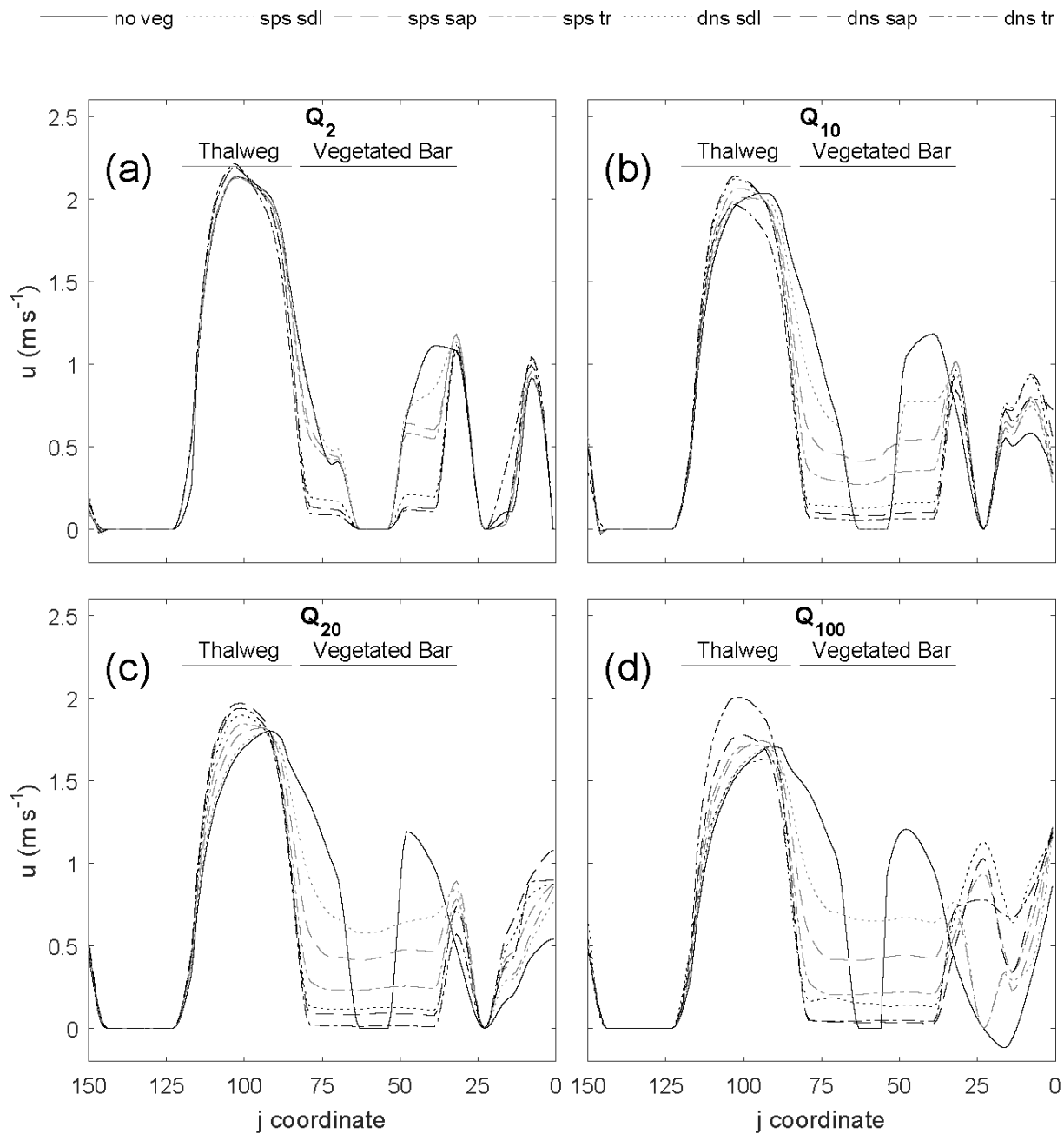


Figure 6. Effect of the vegetated bar ($j = 32\text{--}82$) on the streamwise (u) velocity at the midstream cross section (XS2) for the Q_2 (a), Q_{10} (b), Q_{20} (c), and Q_{100} (d) flows. In the thalweg ($j = 100$), u increases and the maximum shifts toward the left bank. On the bar, velocity is decreased in the patch, and increased at the right edge of the patch.

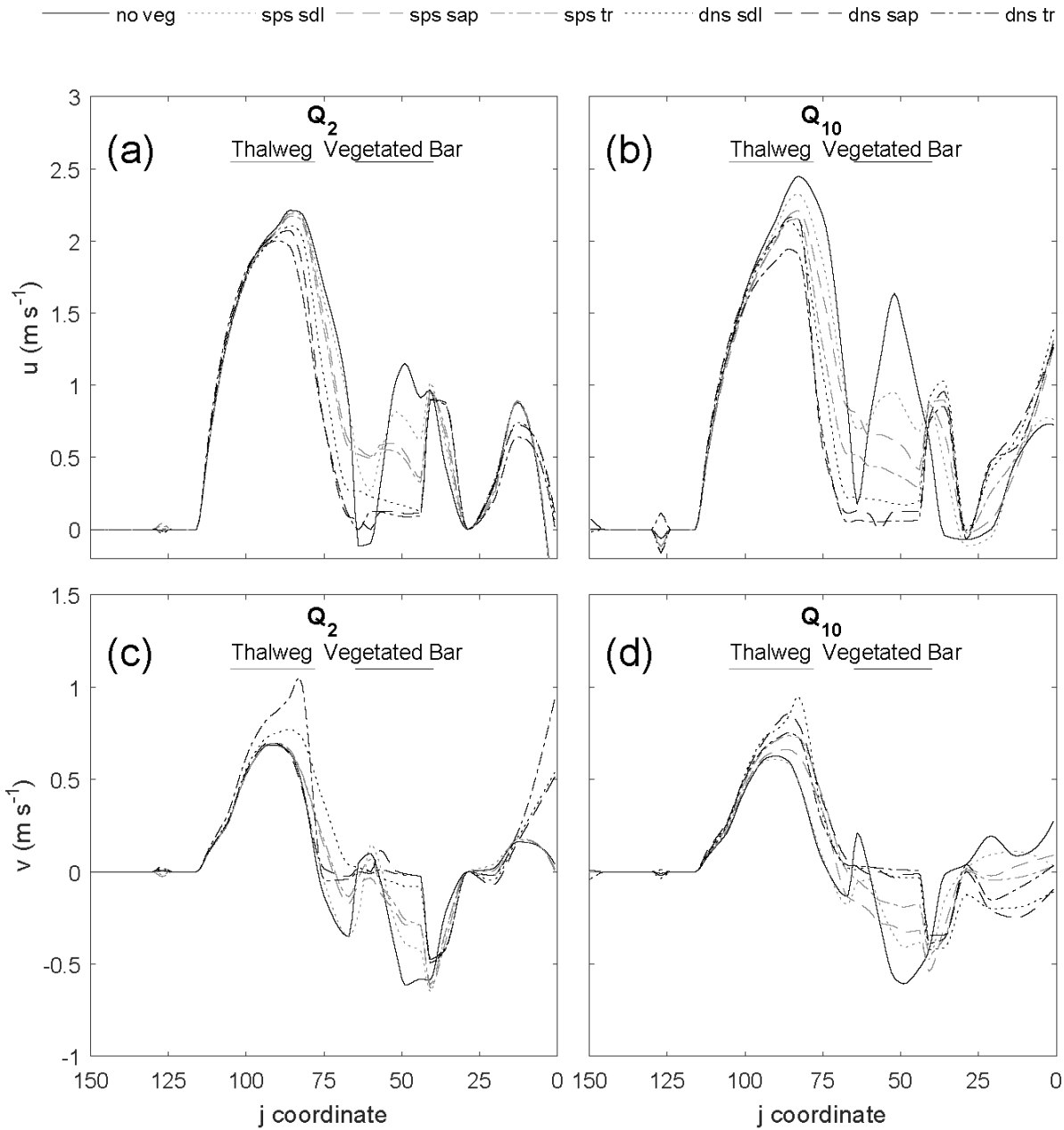


Figure 7. Effect of the vegetated bar ($j = 50-65$) on the streamwise (u ; a,b) and stream-normal (v ; c,d) velocity at the upstream cross section (XS1) for the Q_2 (a,c) and Q_{10} (b,d) flows. In the thalweg ($j = 90$) and at the head of the bar, u is decreased with increasing seedling size and density. For $Q \geq Q_{10}$, v was decreased (became more negative) adjacent to the vegetation patch.

The manner in which different vegetation densities and growth stages influenced hydraulics varied spatially around the bend. In general, adding vegetation increased velocity within the thalweg and at the edge of the vegetation patch compared to the no-vegetation case, creating concentrated flow paths adjacent to the patch while reducing velocity and shear stress at the head of the bar and within the vegetation patch. The effect of the vegetated bar on channel-bend hydraulics became more pronounced with discharges increasing from the Q_2 to Q_{10} . Furthermore, sparse vegetation behaved similarly to the no-vegetation scenario for low flows, but had an increasing effect on hydraulics at the flows $\geq Q_{10}$. Vegetation effects increased steeply from Q_2 to Q_{10} with modest changes thereafter. In general, hydraulics were more sensitive to plant morphology differences (A_c) for sparse conditions compared to dense conditions (Fig. 5, 6, 7).

At the downstream end of the bar (XS1; Fig. 5), vegetation increased the magnitude of downstream (u) and cross-stream (v more negative) velocity within the thalweg region, and reduced velocities over the bar. For flows $\geq Q_{10}$, the high-velocity core became more concentrated and shifted away from the bar. This thalweg effect became more pronounced with increasing plant density and plant size, except in the case of dense young trees, which behaved more similarly to the bare bar scenario for the Q_{10} flow. Amplification of thalweg velocities at XS1 was greatest for the dense sapling scenario, with 17 % and 12 % increases in u and v , respectively, for the Q_{10} , and increases in velocity magnitude for flows $> Q_{10}$. On the vegetated bar, u and v decreased within the vegetated patch, with u values reduced up to 56 % for the sparse young tree scenario, and up to 95 % for the dense scenarios — these magnitudes are well above uncertainty in velocities. With increasing plant size and density, the values of u and v at the right edge of the vegetation patch were greater than or nearly equal to that in the thalweg, with a particularly large increase for dense scenarios. Thus, flow velocities were decreased within the patch, increased adjacent to the patch, and were deflected toward the left bank.

At the midstream position (XS2), downstream velocities (u) in the thalweg region were greater than at XS1. The impact of the vegetation patch on u for XS2 was pronounced, with u increased up to 30 % within the thalweg and the maximum value of u shifted toward the left bank with increasing plant size, density, and discharge (Fig. 6). Like XS1, the thalweg effect reached a maximum for dense saplings at the Q_{10} . As flow increased (Q_{20} and Q_{100}), dense trees had the greatest effect on increasing thalweg u . On the bar, the effect on u for XS2 was similar to XS1. Values of u decreased with increasing size and density of plants, and u increased at the right outer edge of the vegetation patch. Over the bar, u was reduced up to 99 % for the dense scenarios compared to the no-vegetation scenario, and increased at the edge of the patch up to 3300 %. At XS2, v values were small compared to XS1 and XS3 and were relatively insensitive to the presence of the vegetation patch.

At the upstream end of the bar (XS3; Fig. 7), an opposite trend in changes in u within the thalweg was observed. With increasing seedling size and density, u was decreased within the thalweg and at the head of the bar, with a maximum reduction in u of 29 % for dense scenarios. For $Q \geq Q_{10}$, v was more positive to the left (70 %) of the vegetation patch and more negative to the right of the vegetation patch (180 % reduced). Within the vegetation patch, u and v were reduced (96 % and 100 %, respectively). Thus, flow was steered away from the vegetation patch.

4 Discussion

4.1 Impact of vegetation on channel-bend hydraulics

Our results illustrate that vegetation enhances ~~the effects of bars on~~ flow steering ~~on bars~~, complementing previous work on bend dynamics in the absence of vegetation. Dietrich and Smith (1983) showed that bars steered flow in a manner that forced forces the high-velocity core toward the concave bank. They additionally found that flow over the heads of bars resulted in cross-stream components of velocity (v) and boundary shear stress (τ_n) directed toward the concave bank. Laboratory studies by (Blanckaert, (2010), representing sharp meander bends, identified relationships between zones of inward versus outward mass transport, transverse bed profiles, and curvature variations, as well as illustrating that curvature-induced secondary flow associated with topographic steering concentrates most discharge over the deepest, outer parts of a bend. Whiting (1997) hypothesized that convective accelerations arising from flow steering would be most important at low flows, whereas Legleiter et al. (2011) showed that steering from bars continued to be important with increasing discharge. We found that vegetation began to have a detectable impact on channel-bend hydraulics for flows greater than the Q_2 , when plants ~~began to be~~ inundated, ~~and that vegetation-induced alteration of hydraulics was initially steep from Q_2 to Q_{10} , with modest changes thereafter. Vegetation effects on flow did not decrease with increasing discharge, consistent with~~ Similar to Abu-Aly et al. (2014), ~~we found that the influence of vegetation on flow did not decrease with increasing discharge, but stabilized after increased with vegetation inundation flow depths were achieved. This suggests an initial steep increase in alteration of hydraulics from vegetation from Q_2 to Q_{10} , with modest changes thereafter. This furthermore indicates that w~~ Whereas flow steering from bars may be most important at low flows (Whiting, 1997), our results suggest that flow steering will continue to be important over a range of flows for vegetated bars.

In general, we found the impact of the vegetated bar on channel-bend hydraulics to ~~increase vary~~ with both plant density and size morphology, and our modeling illustrated nuances in these relationships of modeled plants modelled. Plant ~~However, m~~ morphology differences affected hydraulics preferentially for sparse cases, whereas dense cases were similar. ~~Some nuances warrant notice. For example, Dd~~ Dense young trees, however, did not always result in the maximum alteration to channel-bend hydraulics—particularly for u during the Q_{10} flow. At the downstream end of the bar, the high-velocity core became more concentrated and shifted away from the bar with increasing plant density and plant size, except in the case of dense young trees. Dense young trees behaved more similarly to the bare bar scenario for the Q_{10} flow. This indicates there may be thresholds whereby increasing density and size of vegetation no longer results in ~~a linear change in an hydraulics~~ additional hydraulic effect in some cases. Together, these results suggest altered bend hydraulics caused by bar vegetation may be most pronounced for vegetation-inundating flows up to Q_{10} under sparse-vegetation conditions. We may expect vegetation-morphodynamic interactions to be strongest as recruited sparse woody riparian vegetation matures under moderate flow conditions ($> Q_2$ to Q_{10}), or conversely, if a bare bar establishes dense vegetation. This is consistent with the biogeomorphic phase concept (Corenblit et al., 2007, 2015a, 2015b), whereby established vegetation has strong feedbacks

with geomorphic processes, but with the additional constraint of enhanced interactions under a specific range of flow magnitudes.

At the mid- and downstream sections of the channel bend investigated, the presence of dense vegetation increased downstream velocity (u) within the thalweg up to 30 % and shifted the high-velocity core toward the cutbank. Vegetation increased the magnitude of cross-stream velocity (v) at both the up- and downstream end of the channel bend by increasing cross-stream flow toward the cutbank at the head of the bar and around the toe of the bar. Positive v values within the thalweg region at the upstream cross section (XS3) indicate, indeed, flow is steered toward the concave bank. By extension, cross-stream shear stress, τ_n is directed toward the concave bank ~~given equation (2)~~. At the head of the bar, flow was additionally slowed within the channel (u decreased), and steered away from the vegetation patch, increasing flow within a side channel adjacent to the bar head and creating concentrated flow paths adjacent to the patch.

We acknowledge that some of our findings may be influenced by limitations of our modeling approach, which reflect persistent challenges in characterizing the complexities of vegetation architecture and flow in a modeling framework. Our analysis simplified vegetation drag by assuming rigid cylinders, which has been found to most accurate for dense vegetation (Vargas-Luna et al., 2016). We used τ_n and by using a constant vegetation drag coefficient, consistent with other studies. This approach likely overestimates vegetation drag at higher discharges, when the canopy is inundated and plants are more streamlined, reducing A_c and $C_{d,v}$ (James et al., 2004). Future research directions include: 1) refining how vegetation drag is represented, especially for sparse vegetation; 2) quantifying changes in drag that result from streamlining and reconfiguration during inundation; 3) including variations in drag coefficient for vegetation to represent depth-dependence and complexities of vegetation architecture; and 4) evaluating effects of non-logarithmic vertical velocity structures (Aberle and Järvelä, 2013; Boothroyd et al., 2017; Nepf, 2012; Västilä et al., 2013; Västilä and Järvelä, 2014; Whittaker et al., 2013).

Some flume and modelling studies support our results, but others illustrate the variability in hydraulic response to vegetation as a function of channel geometry. For example, Marjoribanks et al. (2017) modelled the effects of vegetation on channel hydraulics for a small (~5 m wide by 16 m long), straight river reach and found downstream (u) and cross stream velocities (v) reduced broadly throughout the channel. Here, we found reduction of u and v to vary spatially depending on the location within the channel bend and relative to the vegetation patch. Rominger et al. (2010), working with two reed species planted on the sandy point bar of a constructed, meandering experimental stream, found that vegetation reduced u values over the vegetated bar, increased them in the thalweg, strengthened secondary circulation, and directed secondary flow toward the outer bank. Another study in the same experimental facility, but using woody seedlings planted on the point bar, also found reduced velocities in the vegetated area of the bar, with the greatest reductions at the upstream end, and strengthening of secondary circulation, as well as illustrating differences in hydraulic effects as a result of variations in vegetation architecture and density (Lightbody et al., 2012). In another flume study where meandering was simulated in a straight channel by placing dowels representing vegetation patches in alternating locations along the edges of the flume, vegetation reduced velocity within and at the edges of the vegetation patch and increased velocities near the opposite bank, consistent with the results here (Bennett et al., 2002). However, Termini (2016) considered vegetation's effect on flow in a high-curvature meandering flume and found

that vegetation inhibited high shear stress values from reaching the outer bank, inconsistent with the results found here and in other studies simulating moderate sinuosity channels.

4.2 Implications for channel morphology and evolution

5 The reduction of velocity and shear stress ~~and associated reduction in momentum transfer~~ within the thalweg at the bar head caused by the presence of the vegetated bar would be expected to decrease sediment transport in this region. Van Dijk et al. (2013), in an experimental channel, found bar vegetation to increase fine-sediment deposition upstream of the vegetation patch, analogous to the bar head of our work. This may contribute to bar-head maintenance, such that the head of the bar is not eroded. Maintenance of the bar head would be countered by the potential for chute cutoff (van Dijk et al., 2014) or channel switching
10 that may result because of concentrated flow paths. ~~Along the inside (At the river right) edge of the vegetated bar, a exists a region of lower-elevation, chute-channel-like region is present, in which .In this region,~~ flow was concentrated and velocities increased as vegetation size and density increased. Seedling establishment was not successful in the lower-elevation region during the study period, ~~possibly because higher shear stresses in this region limited fine sediment deposition conducive to recruitment and/or exceeded~~ ~~suggesting~~ uprooting thresholds ~~may be met in this region~~ (Bywater-Reyes et al., 2015). ~~We suggest that, although exaggerated,~~
15 ~~The concentrated flow paths adjacent to the vegetation patch, on the inside of the bar, may be characteristic of~~ ~~represent~~ conditions on vegetated bars along channel bends more generally, where both ridge and swale topography and chute bars may be present (Kleinhans and van den Berg, 2011), and where chute cutoffs and vegetation roughness and cohesion interact to influence morphodynamics (e.g., Braudrick et al., 2009). ~~that likely occur on the bar and other rivers with vegetated bars.~~ Seedlings often recruit along floodlines (Schneider and Moggridge, 2009), forming rows of
20 trees. Low-velocity areas within the rows induce fine-sediment deposition, steering flow away from the rows, and increasing velocity and shear stress adjacent to the rows such that sediment is transported in these regions. This process has been invoked to explain how vegetation creates vegetated islands (Gurnell et al., 2001), alternating patterns of vegetated ridges and adjacent channels (Tooth and Nanson, 2000), and the evolution of anabranching channels (Tooth et al., 2008). Van Dijk et al. (2013) found flood-dispersed vegetation recruited on bars resulted in island braiding, whereas vegetation distributed uniformly across
25 the floodplain maintained a single-thread meandering channel with increased sinuosity and decreased bend wavelength. Our analysis, more comparable to the flood-dispersed case, shows the potential for development of vegetated islands, but also for prevention of chute cutoff through bar-head maintenance; ~~chute cutoff may be more likely in the absence of vegetation~~ (Constantine et al., 2010).

The production of a low-velocity region over the vegetated bar could increase fine-sediment deposition on the bar,
30 consistent with flume and field observations. Elevated sediment deposition within patches of woody seedlings, with variations depending on plant characteristics, has been documented in meandering (Kui et al., 2014) and straight (Diehl et al., 2017b) flumes. Gorrick and Rodríguez (2012), working in a flume in which vegetation patches were simulated with dowels, documented elevated fine-sediment deposition within the patches (Gorrick and Rodríguez, 2012). Zones of fine sediment

deposition on bars associated with roughness from vegetation or instream wood can in turn create sites for plant germination and seedling growth (e.g., Gurnell and Petts, 2006). At our field site, we developed a grain size patch map (Buffington and Montgomery, 1999) on the vegetated bar, which illustrates an obvious correlation between sandy patches and the location of trees that have experienced several floods (Fig. 8). If reduced velocities result in increased deposition of sediment on the bar, bar accretion would induce additional topographic steering. This feedback would be expected to accelerate channel migration rates. would also contribute to bar building, imposing an additional feedback as topographic steering from the bar is enhanced.

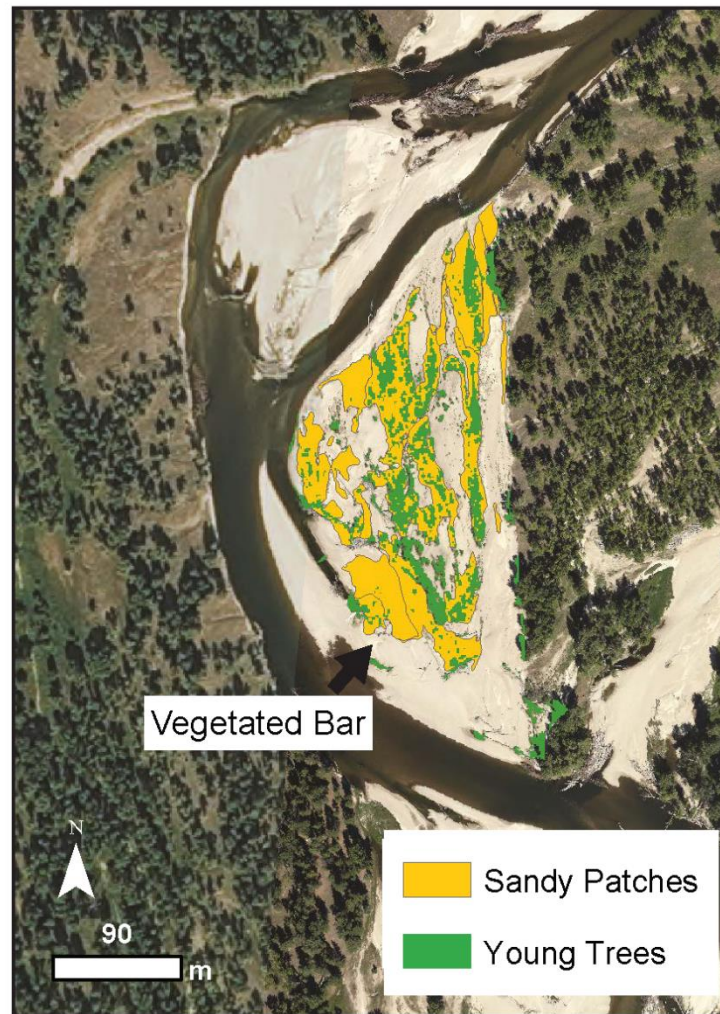


Figure 8. The vegetated bar, showing the spatial co-occurrence of sandy grain size patches and young trees (extracted from aerial imagery).

10

The increase in velocity and shift of the high velocity core toward the cutbank combined with low velocities within the vegetation patch would create a large velocity gradient across the channel. A larger velocity gradient within the thalweg

compared to over the bar would be expected to alter the dynamics of bank erosion. As a simple rule, bank erosion rate, \dot{n} , according to Parker et al.'s (2011) HIPS model is proportional to an erosion coefficient, k , and half the streamwise velocity difference between the two banks, Δu :

$$\dot{n} = k\Delta u \quad (35)$$

5 The parameter, k , represents the material cohesion and vegetation root properties that control bank erosion and varies between 10^{-8} and 10^{-7} (dimensionless). ~~Thus, for an assumed k , vegetation-induced velocity gradients across the channel are expected to alter bank erosion rates. Thus, although we show the potential for concentrated flow paths to cause a morphology with vegetated islands, our analysis does not preclude bar vegetation from increasing bank erosion rates that would tend to increase sinuosity, in contrast to previous experimental work suggesting flood-established vegetation should result in island development (Van Dijk et al., 2013).~~

10 Vegetation “pushing” flow toward the outer bank is analogous to “bar push” (Allmendinger et al., 2005; Parker et al., 2011), whereby a rapidly accreting point bar may cause erosion at the outer bank (Eke et al., 2014; van de Lageweg et al., 2014). This increase in bank erosion would be countered by deposition of fine sediment on the bar resulting from the vegetation-induced reduction in velocity in this region, that may in turn induce addition “push” through bar building (e.g., Eke et al., 2014). Coarse bank roughness counters this effect, pushing the high velocity core back toward the center of the channel (Gorrick and Rodríguez, 2012; Thorne and Furbish, 1995). The balance between erosion of the bank and deposition on the bar would thus dictate whether net erosion or net deposition within the active channel occurs, inducing changes in channel width (Eke et al., 2014), and altering channel morphology.

20 ~~Width to depth ratios higher and lower than expected based on at a station hydraulic geometry have been reported for vegetated channels (Corenblit et al., 2007). Initial riparian forest development may result in a decrease in width to depth ratio as formerly bare banks are vegetated and increase bank cohesion, preventing bank erosion from widening channels (Métivier and Barrier, 2012) such that meanders (Eaton and Giles, 2009) and alternate bars emerge (Kleinhans, 2010). For channels characterized by vegetated banks and meandering planforms, differences in width have been observed based on floodplain and bank vegetation type, with floodplains composed of herbaceous vegetation associated with narrower channels compared to those composed of woody vegetation (Allmendinger et al., 2005; Hession et al., 2003; Jackson et al., 2015). It is unclear what would cause this relationship, since bank strength increases with rooting depth (Eaton and Giles, 2009), which is greater for woody vegetation compared to herbaceous vegetation (Canadell et al., 1996). Our site has woody vegetation on banks and floodplains, and has both bars with abundant vegetation (Bar 1) and those relatively free of vegetation (Bar 2, Bar 3; Fig. 1). Comparison of the morphology of the vegetated bar at the site to two others with very little vegetation (2012 topography; Fig. 9) shows that the bars had similar widths, but the vegetated bar (Bar 1) had a deeper thalweg. This may be a manifestation of increased, concentrated velocity and shear stress in this region. This suggests the vegetated bar had a smaller width to depth ratio compared to the others, inconsistent with the notion that floodplains composed of herbaceous vegetation are associated with narrower channels compared to those composed of woody vegetation (Allmendinger et al., 2005; Hession et al., 2003; Jackson et al., 2015).~~

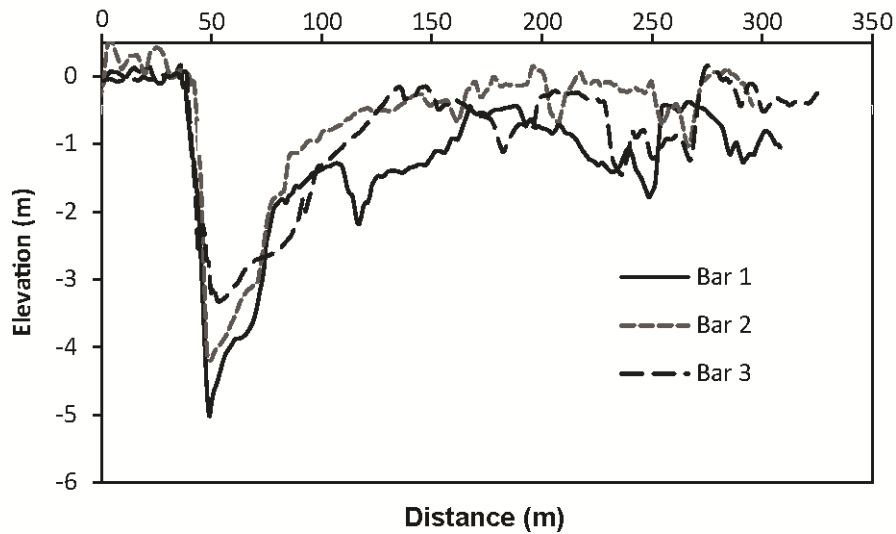


Figure 9. Cross sections for the vegetated bar (Bar 1), and two others (locations shown in Fig. 1). The vegetated bar (Bar 1) has a deeper thalweg compared to the other two bars, but similar widths. Note the horizontal axis for Bar 3 has been reversed for comparison of geometry.

5

However, the width to depth ratio of a channel should adjust depending on the outcome of bars and vegetation “pushing” banks, versus bar accretion. On the one hand, vegetation may decrease width to depth ratios from a combination of increased bank strength and scouring deeper thalwegs because of concentrated flow around the bend. On the other, concentrated streamwise flow paths at the head of the bar combined with a shift in the high velocity core toward the cutbank, large differential in cross stream velocities, and cross stream accelerations would tend to increase bank erosion at the mid and downstream end that may be accompanied by bank pull bar building.

10

5 Conclusion

The presence of a vegetated bar in a gravel-bed river altered both streamwise and cross-stream components of velocity vectors for overbank flows, with an increasing effect with discharge and both plant density and size. Vegetation steered flow away from the vegetated bar, creating concentrated flow paths in surrounding low-elevation side channels and a low-velocity region over the vegetated patch. Flow was slowed at the apex of the bar, and increased within the thalweg around the bend. These changes in hydraulics are expected to could increase fine sediment deposition on the bar, potentially creating hospitable sites for vegetation recruitment, and increasing bank erosion that is dependent on cross-stream velocity gradients. This pattern would tend to reduce cross-stream sediment transport at the bar head, but increase it around the remainder of the bend.

20

Our analysis simplified vegetation drag by assuming rigid cylinders, and recent research has suggested this is most accurate for dense vegetation (Vargas Luna et al., 2016). Future research directions include refining how vegetation drag is represented for sparse vegetation, as well as quantifying changes in drag that result from streamlining and reconfiguration during inundation (Aberle and Järvelä, 2013; Boothroyd et al., 2017; Nepf, 2012; Västilä et al., 2013; Västilä and Järvelä, 2014; Whittaker et al., 2013). As we have represented vegetation (as rigid cylinders), we likely overestimate vegetation drag at higher discharges when the canopy is inundated and plants are more streamlined. Furthermore, we used a constant vegetation drag coefficient and a logarithmic profile for all vegetation scenarios. Streamlining, in addition to reducing A_c , would reduce $C_{d,v}$ (James et al., 2004). An expansion of this research could consider vegetation streamlining, a drag coefficient dependent on flow conditions, and more complex vertical velocity structure.

Following the patterns of hydraulics and forces, we would expect vegetation to change the morphodynamic evolution of channels with vegetation pushing flow in a manner previously only typically attributed to bars, and increasing bank erosion rates, and may explain the enigmatic observation that reaches characterized by woody vegetation are wider than those with herbaceous vegetation. Subsequent bank retreat may induce bar building, which would could be accelerated by fine-sediment deposition within the vegetation patch. This feedback would induce additional topographic steering from the presence of the bar. With a numerical model, we have characterized a mechanisms by which channels with vegetated bars may evolve different morphologies and rates compared to those without, thereby contributing to understanding of ecogeomorphic feedbacks in river-floodplain systems (Gurnell, 2014) and of how life influences landscapes (Dietrich and Perron, 2006).

List of terms

- 20 A_c = vegetation frontal area (m^2)
 ~~A_s = frontal area of stems (m^2)~~
 C_d = channel drag coefficient
 $C_{d,v}$ = vegetation drag coefficient
 D = median grain size (m)
- 25 F_D = vegetation drag ($N m^{-2}$)
 g = acceleration due to gravity ($m s^{-2}$)
 k = bank erosion coefficient
 u = streamwise component of velocity ($m s^{-1}$)
 \bar{U} = depth-averaged velocity ($m s^{-1}$)
- 30 U_x = x component of velocity in Cartesian coordinate system ($m s^{-1}$)
 U_y = y component of boundary velocity in Cartesian coordinate system ($m s^{-1}$)
 U_c = approach velocity ($m s^{-1}$)
 ~~U_m = cross section mean velocity ($m s^{-1}$)~~
 v = stream-normal component of velocity ($m s^{-1}$)

ρ = density of water (kg m^{-3})

ρ_s = density of sediment (kg m^{-3})

τ = boundary shear stress (N m^{-2})

τ^* = Shields number

5 τ_x = stream wise component of boundary shear stress (N m^{-2})

τ_n = stream normal component of boundary shear stress (N m^{-2})

\dot{n} = bank erosion rate

10 Data availability

Please inquire with Missoula County for aerial LiDAR. Ground-based LiDAR is available at <https://tls.unavco.org/projects/U-026/>; Bitterroot Site 1 DOI: 10.7283/R34M07; Bitterroot Site 2 DOI: 10.7283/R30W61, Bitterroot Site 3 DOI: 10.7283/R3W62P. FaSTMECH solver files are available upon request.

15 Author contribution

S. Bywater-Reyes and A.C. Wilcox designed the ~~modelling~~ modeling experiment. R.M. Diehl contributed to updating FaSTMECH code to account for vegetation drag. S. Bywater-Reyes carried out field work and model construction, calibration, and implementation. S. Bywater-Reyes wrote the manuscript with contributions ~~from~~ all co-authors.

20 Acknowledgements

This research was funded by the National Science Foundation (EAR-1024652, EPS-1101342) and EPA STAR Graduate Fellowship. We thank Mark Reiling, Philip Ramsey and MPG Ranch for access to the Bitterroot site. We thank Missoula County for providing LiDAR. We thank Sarah Doelger and UNAVCO, Austin Maphis, Katie Monaco, April Sawyer, and John Bowes for assistance in the field. A special thanks to Carl Legleiter for sharing his scripts and Richard McDonald, Gregory Pasternack, Daniele Tonina, David Machač, Nicholas Silverman, and Doug Brugger for ~~modelling~~ modeling and scripting tips. The Mexcgns-Matlab scripts used in this study are available upon request of the first author.

Supplement

Supporting experimental procedures can be found in the supplement

30 References

Aberle, J. and Järvelä, J.: Flow resistance of emergent rigid and flexible floodplain vegetation, J. Hydraul. Res., 51(1), 33–45, doi:10.1080/00221686.2012.754795, 2013.

- Abu-Aly, T. R., Pasternack, G. B., Wyrick, J. R., Barker, R., Massa, D. and Johnson, T.: Effects of LiDAR-derived, spatially distributed vegetation roughness on two-dimensional hydraulics in a gravel-cobble river at flows of 0.2 to 20 times bankfull, *Geomorphology*, 206, 468–482, doi:10.1016/j.geomorph.2013.10.017, 2014.
- Allmendinger, N. E., Pizzuto, J. E., Potter, N., Johnson, T. E. and Hession, W. C.: The influence of riparian vegetation on stream width, eastern Pennsylvania, USA, *Geol. Soc. Am. Bull.*, 117(1), 229–243, doi:10.1130/B25447.1, 2005.
- Amlin, N. M. and Rood, S. B.: Comparative tolerances of riparian willows and cottonwoods to water-table decline, *Wetlands*, 22(2), 338–346, 2002.
- Antonarakis, A. S., Richards, K. S., Brasington, J. and Muller, E.: Determining leaf area index and leafy tree roughness using terrestrial laser scanning, *Water Resour. Res.*, 46(6), W06510, doi:10.1029/2009WR008318, 2010.
- 10 Asahi, K., Shimizu, Y., Nelson, J. and Parker, G.: Numerical simulation of river meandering with self-evolving banks, *J. Geophys. Res. Earth Surf.*, 118(February), 1–22, doi:10.1002/jgrf.20150, 2013.
- Baptist, M., Bosch, L. van den, Dijkstra, J. T. and Kapinga, S.: Modelling the effects of vegetation on flow and morphology in rivers, in *Large Rivers*, vol. 15, pp. 339–357, *Arch. Hydrobiol.*, 2005.
- Baptist, M., Babovic, V., Rodríguez, J., Keijzer, M., Uittenbogaard, R., Mynett, A. and Verwey, A.: On inducing equations for vegetation resistance, *J. Hydraul. Res.*, 45(4), 435–450, 2007.
- 15 Bendix, J. and Hupp, C.: Hydrological and geomorphological impacts on riparian plant communities, *Hydrol. Process.*, 14, 2977–2990, 2000.
- Bennett, S. J., Pirim, T. and Barkdoll, B. D.: Using simulated emergent vegetation to alter stream flow direction within a straight experimental channel, *Geomorphology*, 44(1–2), 115–126, 2002.
- 20 Bertoldi, W. and Siviglia, A.: Modeling vegetation controls on fluvial morphological trajectories, *Geophys. Res. Lett.*, 41, 1–9, doi:10.1002/2014GL061666, 2014.
- Blanckaert, K.: Topographic steering, flow recirculation, velocity redistribution, and bed topography in sharp meander bends, *Water Resour. Res.*, 46(9), 1–23, doi:10.1029/2009WR008303, 2010.
- Blondeaux, P. and Seminara, G.: A unified bar-bend theory of river meanders, *J. Fluid Mech.*, 157, 449–470, 1985.
- 25 Boothroyd, R. J., Hardy, R. J., Warburton, J. and Marjoribanks, T. I.: The importance of accurately representing submerged vegetation morphology in the numerical prediction of complex river flow, *Earth Surf. Process. Landforms*, 41, 567–576, doi:10.1002/esp.3871, 2016.
- Boothroyd, R. J., Hardy, R. J., Warburton, J. and Marjoribanks, T. I.: Modeling complex flow structures and drag around a submerged plant of varied posture, *Water Resour. Res.*, 53, 2877–2901, doi:10.1002/2016WR020186, 2017.
- Boyd, K., Thatcher, T. and Kellogg, W.: Musselshell River Watershed Plan, , (September), 131, 2015.
- 30 Braudrick, C. A., Dietrich, W. E., Leverich, G. T. and Sklar, L. S.: Experimental evidence for the conditions necessary to sustain meandering in coarse-bedded rivers., *Proc. Natl. Acad. Sci. U. S. A.*, 106(40), 16936–41, doi:10.1073/pnas.0909417106, 2009.
- Bywater-Reyes, S., Wilcox, A. C., Stella, J. C. and Lightbody, A. F.: Flow and scour constraints on uprooting of pioneer woody seedlings, *Water Resour. Res.*, 51(11), 9190–9206, doi:10.1002/2014WR016641, 2015.
- Bywater-Reyes, S., Wilcox, A. C. and Diehl, R. M.: Multiscale influence of woody riparian vegetation on fluvial topography quantified with ground-based and airborne lidar, *J. Geophys. Res. Earth Surf.*, 122(6), 1218–1235, doi:10.1002/2016JF004058, 2017.
- 35 Camporeale, C., Perucca, E., Ridolfi, L. and Gurnell, A.: Modeling the interactions between river morphodynamics and riparian vegetation, *Rev. Geophys.*, 51, 1–36, doi:10.1002/rog.20014, 2013.
- Constantine, J. A., McLean, S. R. and Dunne, T.: A mechanism of chute cutoff along large meandering rivers with uniform floodplain

- topography, *Geol. Soc. Am. Bull.*, 122, 855–869, doi:10.1130/B26560.1, 2010.
- Corenblit, D., Tabacchi, E., Steiger, J. and Gurnell, A. M.: Reciprocal interactions and adjustments between fluvial landforms and vegetation dynamics in river corridors: A review of complementary approaches, *Earth-Science Rev.*, 84, 56–86, doi:10.1016/j.earscirev.2007.05.004, 2007.
- 5 Corenblit, D., Davies, N. S., Steiger, J., Gibling, M. R. and Bornette, G.: Considering river structure and stability in the light of evolution: feedbacks between riparian vegetation and hydrogeomorphology, *Earth Surf. Process. Landforms*, 40(September 2014), 189–207, doi:10.1002/esp.3643, 2015a.
- Corenblit, D., Baas, A., Balke, T., Bouma, T., Fromard, F., Garófano-Gómez, V., González, E., Gurnell, A. M., Hortobágyi, B., Julien, F., Kim, D., Lambs, L., Stallins, J. A., Steiger, J., Tabacchi, E. and Walcker, R.: Engineer pioneer plants respond to and affect geomorphic constraints similarly along water-terrestrial interfaces world-wide, *Glob. Ecol. Biogeogr.*, 1–14, doi:10.1111/geb.12373, 2015b.
- 10 Curran, J. C. and Hession, W. C.: Vegetative impacts on hydraulics and sediment processes across the fluvial system, *J. Hydrol.*, 505, 364–376, doi:10.1016/j.jhydrol.2013.10.013, 2013.
- Dean, D. J. and Schmidt, J. C.: The role of feedback mechanisms in historic channel changes of the lower Rio Grande in the Big Bend region, *Geomorphology*, 126, 333–349, doi:10.1016/j.geomorph.2010.03.009, 2011.
- 15 Diehl, R. M., Merritt, D. M., Wilcox, A. C. and Scott, M. L.: Applying functional traits to ecogeomorphic processes in riparian ecosystems, *Bioscience*, 67(8), 729–743, doi:10.1093/biosci/bix080, 2017a.
- Diehl, R. M., Wilcox, A. C., Stella, J. C., Kui, L., Sklar, L. S. and Lightbody, A.: Fluvial sediment supply and pioneer woody seedlings as a control on bar-surface topography, *Earth Surf. Process. Landforms*, 42(5), 724–734, doi:10.1002/esp.4017, 2017b.
- Dietrich, W. E. and Perron, J. T.: The search for a topographic signature of life, *Nature*, 439, 411–418, doi:10.1038/nature04452, 2006.
- 20 Dietrich, W. E. and Smith, J. D.: Influence of the point bar on flow through curved channels, *Water Resour. Res.*, 19(5), 1173–1192, 1983.
- Dietrich, W. E. and Whiting, P.: Boundary shear stress and sediment transport in river meanders of sand and gravel, in *River Meandering*. AGU Water Resources Monograph 12, edited by S. Ikeda and G. Parker, pp. 1–50, American Geophysical Union, Washington DC., 1989.
- van Dijk, W. M., Schuurman, F., van de Lageweg, W. I. and Kleinhans, M. G.: Bifurcation instability and chute cutoff development in meandering gravel-bed rivers, *Geomorphology*, 213, 277–291, doi:10.1016/j.geomorph.2014.01.018, 2014.
- 25 Van Dijk, W. M., Teske, R., Van De Lageweg, W. I. and Kleinhans, M. G.: Effects of vegetation distribution on experimental river channel dynamics, *Water Resour. Res.*, 49(11), 7558–7574, doi:10.1002/2013WR013574, 2013.
- Eke, E., Parker, G. and Shimizu, Y.: Numerical modeling of erosional and depositional bank processes in migrating river bends with self-formed width: Morphodynamics of bar push and bank pull, *J. Geophys. Res. Earth Surf.*, 119, 1455–1483, doi:10.1002/2013JF003020, 2014.
- Gorrick, S. and Rodríguez, J. F.: Sediment dynamics in a sand bed stream with riparian vegetation, *Water Resour. Res.*, 48(2), 1–15, doi:10.1029/2011WR011030, 2012.
- 30 Gran, K. and Paola, C.: Riparian vegetation controls on braided stream dynamics, *Water Resour. Res.*, 37(12), 3275–3283 [online] Available from: http://nced.umn.edu/system/files/2010sicm_gran2001.pdf (Accessed 2 February 2012), 2001.
- Green, J. C.: Modelling flow resistance in vegetated streams: Review and development of new theory, *Hydrol. Process.*, 19, 1245–1259, doi:10.1002/hyp.5564, 2005.
- 35 Gurnell, A.: Plants as river system engineers, *Earth Surf. Process. Landforms*, 39, 4–25, doi:10.1002/esp.3397, 2014.
- Gurnell, A. and Petts, G.: Trees as riparian engineers: the Tagliamento River, Italy, *Earth Surf. Process. Landforms*, 1574(May), 1558–1574, doi:10.1002/esp, 2006.
- Gurnell, A. M., Petts, G. E., Hannah, D. M., Smith, B. P. G., Edwards, P. J., Kollmann, J., Ward, J. V. and Tockner, K.: Riparian vegetation

- and island formation along the gravel-bed Fiume Tagliamento, Italy, *Earth Surf. Process. Landforms*, 26(1), 31–62, doi:10.1002/1096-9837(200101)26:1<31::AID-ESP155>3.0.CO;2-Y, 2001.
- Ikeda, S., Parker, G. and Sawai, K.: Bend theory of river meanders. Part 1. Linear development, *J. Fluid Mech.*, 112, 363–377, doi:10.1017/S0022112081000451, 1981.
- 5 Iwasaki, T., Shimizu, Y. and Kimura, I.: Numerical simulation of bar and bank erosion in a vegetated floodplain: A case study in the Otofuke River, *Adv. Water Resour.*, doi:10.1016/j.advwatres.2015.02.001, 2015.
- Jalonen, J., Järvelä, J. and Aberle, J.: Leaf area index as vegetation density measure for hydraulic analyses, *J. Hydraul. Eng.*, 139(5), 461–469, doi:10.1061/(ASCE)HY.1943-7900.0000700, 2013.
- James, C., Birkhead, A. and Jordanova, A.: Flow resistance of emergent vegetation, *J. Hydraul. Res.*, 42(4), 37–41, 2004.
- 10 Karrenberg, S., Edwards, P. and Kollmann, J.: The life history of Salicaceae living in the active zone of floodplains, *Freshw. Biol.*, 47(4), 733–748, 2002.
- Kleinhans, M. G. and van den Berg, J. H.: River channel and bar patterns explained and predicted by an empirical and a physics-based method, *Earth Surf. Process. Landforms*, 36(6), 721–738, doi:10.1002/esp.2090, 2011.
- Kui, L., Stella, J., Lightbody, A. and Wilcox, A. C.: Ecogeomorphic feedbacks and flood loss of riparian tree seedlings in meandering
15 channel experiments, *Water Resour. Res.*, 50, 9366–9384, doi:10.1002/2014WR015719., 2014.
- van de Lageweg, W. I., van Dijk, W. M., Baar, a. W., Rutten, J. and Kleinhans, M. G.: Bank pull or bar push: What drives scroll-bar formation in meandering rivers?, *Geology*, 42(4), 319–322, doi:10.1130/G35192.1, 2014.
- Legleiter, C. J., Harrison, L. R. and Dunne, T.: Effect of point bar development on the local force balance governing flow in a simple, meandering gravel bed river, *J. Geophys. Res.*, 116(F1), F01005, doi:10.1029/2010JF001838, 2011.
- 20 Lightbody, A., Skorko, K., Kui, L., Stella, J. . and Wilcox, A. .: Hydraulic and topographic response of sand-bed rivers to woody riparian seedlings: field-scale laboratory methods and results, in 2012 Fall Meeting, AGU, San Fransisco, Calif., 3-7 Dec., vol. Abstract E, San Fransisco., 2012.
- Manners, R., Schmidt, J. and Wheaton, J. M.: Multiscalar model for the determination of spatially explicit riparian vegetation roughness, *J. Geophys. Res. Earth Surf.*, 118(1), 65–83, doi:10.1029/2011JF002188, 2013.
- 25 Manners, R. B., Wilcox, A. C., Kui, L., Lightbody, A. F., Stella, J. C. and Sklar, L. S.: When do plants modify fluvial processes? Plant-hydraulic interactions under variable flow and sediment supply rates, *J. Geophys. Res. Earth Surf.*, 120(2), 325–345, doi:10.1002/2014JF003265, 2015.
- Marjoribanks, T. I., Hardy, R. J., Lane, S. N. and Tancock, M. J.: Patch-scale representation of vegetation within hydraulic models, *Earth Surf. Process. Landforms*, 42(5), 699–710, doi:10.1002/esp.4015, 2017.
- 30 Mueller, E. R. and Pitlick, J.: Sediment supply and channel morphology in mountain river systems: 2. Single thread to braided transitions, *J. Geophys. Res. Earth Surf.*, 119(7), 1516–1541, doi:10.1002/2013JF003045, 2014.
- Murray, A. B. and Paola, C.: Modelling the effect of vegetation on channel pattern in bedload rivers, *Earth Surf. Process. Landforms*, 28(2), 131–143, doi:10.1002/esp.428, 2003.
- Nelson, J. M.: iRIC Software: FaSTMECH solver manual, , 1–36, 2013.
- 35 Nelson, J. M. and Smith, J. D.: Flow in meandering channels with natural topography, in *River Meandering*, *Water Resour. Monogr.*, vol. 12, edited by S. Ikeda and G. Parker, pp. 69–102, AGU, Washington DC., 1989.
- Nelson, J. M., Bennett, J. P. and Wiele, S. M.: Flow and sediment-transport modeling, in *Tools in Fluvial Geomorphology*, edited by G. M. Kondolf and H. Piégay, pp. 539–576, Wiley, Chichester., 2003.

- Nelson, J. M., Shimizu, Y., Abe, T., Asahi, K., Gamou, M., Inoue, T., Iwasaki, T., Kakinuma, T., Kawamura, S., Kimura, I., Kyuka, T., McDonald, R. R., Nabi, M., Nakatsugawa, M., Simões, F. R., Takebayashi, H. and Watanabe, Y.: The international river interface cooperative: Public domain flow and morphodynamics software for education and applications, *Adv. Water Resour.*, 93, 62–74, doi:10.1016/j.advwatres.2015.09.017, 2016.
- 5 Nepf, H., Rominger, J. and Zong, L.: Coherent flow structures in vegetated channels, in *Coherent Flow Structures at Earth's Surface*, edited by J. G. Venditti, J. L. Best, M. Church, and R. J. Hardy, pp. 135–147, Wiley-Blackwell., 2013.
- Nepf, H. M.: Drag, turbulence, and diffusion in flow through emergent vegetation, *Water Resour. Res.*, 35(2), 479–489, doi:10.1029/1998WR900069, 1999.
- Nepf, H. M.: Hydrodynamics of vegetated channels, *J. Hydraul. Res.*, 503(3), 262–279, doi:10.1080/00221686.2012.696559, 2012.
- 10 Nicholas, A. P., Ashworth, P. J., Sambrook Smith, G. H. and Sandbach, S. D.: Numerical simulation of bar and island morphodynamics in anabranching megarivers, *J. Geophys. Res. Earth Surf.*, 118, 1–26, doi:10.1002/jgrf.20132, 2013.
- van Oorschot, M., Kleinhans, M., Geerling, G. and Middelkoop, H.: Distinct patterns of interaction between vegetation and morphodynamics, *Earth Surf. Process. Landforms*, 41(6), 791–808, doi:10.1002/esp.3864, 2016.
- Osterkamp, W. R. and Hupp, C. R.: Fluvial processes and vegetation — Glimpses of the past, the present, and perhaps the future, *Geomorphology*, 116(3–4), 274–285, doi:10.1016/j.geomorph.2009.11.018, 2010.
- 15 Osterkamp, W. R., Hupp, C. R. and Stoffel, M.: The interactions between vegetation and erosion: New directions for research at the interface of ecology and geomorphology, *Earth Surf. Process. Landforms*, 37, 23–36, doi:10.1002/esp.2173, 2012.
- Parker, G., Shimizu, Y., Wilkerson, G. V., Eke, E. C., Abad, J. D., Lauer, J. W., Paola, C., Dietrich, W. E. and Voller, V. R.: A new framework for modeling the migration of meandering rivers, *Earth Surf. Process. Landforms*, 36(1), 70–86, doi:10.1002/esp.2113, 2011.
- 20 Pasternack, G. B.: 2D modeling and ecohydraulic analysis, University of California at Davis., 2011.
- Rominger, J. T., Lightbody, A. F., Nepf, H. M. and others: Effects of added vegetation on sand bar stability and stream hydrodynamics, *J. Hydraul. Eng.*, 136(12), 994–1002, doi:10.1061/ASCE?HY.1943-7900.0000215, 2010.
- Rood, S. B., Kalischuk, A. R. and Mahoney, J. M.: Initial cottonwood seedling recruitment following the flood of the century of the Oldman River, Alberta, Canada, *Wetlands*, 18(4), 557–570, 1998.
- 25 Schnauder, I. and Moggridge, H. L.: Vegetation and hydraulic-morphological interactions at the individual plant, patch and channel scale, *Aquat. Sci.*, 71(3), 318–330, doi:10.1007/s00027-009-9202-6, 2009.
- Segura, C. and Pitlick, J.: Coupling fluvial-hydraulic models to predict gravel transport in spatially variable flows, *J. Geophys. Res. Earth Surf.*, 120, 834–855, doi:10.1002/2014JF003302, 2015.
- Straatsma, M. W., Warmink, J. J. and Middelkoop, H.: Two novel methods for field measurements of hydrodynamic density of floodplain vegetation using terrestrial laser scanning and digital parallel photography, *Int. J. Remote Sens.*, 29(5), 1595–1617, doi:10.1080/01431160701736455, 2008.
- 30 Termini, D.: Experimental analysis of the effect of vegetation on flow and bed shear stress distribution in high-curvature bends, *Geomorphology*, 274, 1–10, doi:10.1016/j.geomorph.2016.08.031, 2016.
- Thorne, S. D. and Furbish, D. J.: Influences of coarse bank roughness on flow within a sharply curved river bend, *Geomorphology*, 12(3), 241–257, doi:10.1016/0169-555X(95)00007-R, 1995.
- 35 Tonina, D. and Jorde, K.: Hydraulic modeling approaches for ecohydraulic studies: 3D , 2D , 1D and non-numerical models, in *Ecohydraulics: An Integrated Approach*, pp. 31–74., 2013.
- Tooth, S. and Nanson, G. C.: The role of vegetation in the formation of anabranching channels in an ephemeral river, Northern plains, arid

- central Australia, *Hydrol. Process.*, 3117(May 1999), 3099–3117 [online] Available from: [http://onlinelibrary.wiley.com/doi/10.1002/1099-1085\(200011/12\)14:16/17%3C3099::AID-HYP136%3E3.0.CO;2-4/abstract](http://onlinelibrary.wiley.com/doi/10.1002/1099-1085(200011/12)14:16/17%3C3099::AID-HYP136%3E3.0.CO;2-4/abstract) (Accessed 2 February 2012), 2000.
- Tooth, S., Jansen, J. D., Nanson, G. C., Coulthard, T. J. and Pietsch, T.: Riparian vegetation and the late Holocene development of an anabranching river: Magela Creek, northern Australia, *Geol. Soc. Am. Bull.*, 120(7–8), 1021–1035, doi:10.1130/B26165.1, 2008.
- 5 Vargas-Luna, A., Crosato, A. and Uijttewaal, W. S. J.: Effects of vegetation on flow and sediment transport: Comparative analyses and validation of predicting models, *Earth Surf. Process. Landforms*, 40, 157–176, doi:10.1002/esp.3633, 2015.
- Vargas-Luna, A., Crosato, A., Calvani, G. and Uijttewaal, W. S. J.: Representing plants as rigid cylinders in experiments and models, *Adv. Water Resour.*, 93, 205–222, doi:10.1016/j.advwatres.2015.10.004, 2016.
- Västilä, K. and Järvelä, J.: Modeling the flow resistance of woody vegetation using physically-based properties of the foliage and stem,
10 *Water Resour. Res.*, 50, 1–17, doi:10.1002/2013WR013819, 2014.
- Västilä, K., Järvelä, J. and Aberle, J.: Characteristic reference areas for estimating flow resistance of natural foliated vegetation, *J. Hydrol.*, 492, 49–60, doi:10.1016/j.jhydrol.2013.04.015, 2013.
- Wang, C., Wang, Q., Meire, D., Ma, W., Wu, C., Meng, Z., Van de Koppel, J., Troch, P., Verhoeven, R., De Mulder, T. and Temmerman, S.: Biogeomorphic feedback between plant growth and flooding causes alternative stable states in an experimental floodplain, *Adv. Water Resour.*, 93, 223–235, doi:10.1016/j.advwatres.2015.07.003, 2016.
- 15 Whiting, P. J.: The effect of stage on flow and components of the local force balance, *Earth Surf. Process. Landforms*, 22(6), 517–530, doi:10.1002/(SICI)1096-9837(199706)22:6<517::AID-ESP707>3.0.CO;2-M, 1997.
- Whittaker, P., Wilson, C., Aberle, J., Rauch, H. P. and Xavier, P.: A drag force model to incorporate the reconfiguration of full-scale riparian trees under hydrodynamic loading, *J. Hydraul. Res.*, 51(5), 569–580, doi:10.1080/00221686.2013.822936, 2013.
- 20 Wilcox, A. C. and Shafroth, P. B.: Coupled hydrogeomorphic and woody-seedling responses to controlled flood releases in a dryland river, *Water Resour. Res.*, 49(April), n/a-n/a, doi:10.1002/wrcr.20256, 2013.
- Wintenberger, C. L., Rodrigues, S., Bréhéret, J.-G. and Villar, M.: Fluvial islands: First stage of development from nonmigrating (forced) bars and woody-vegetation interactions, *Geomorphology*, 246, 305–320, doi:10.1016/j.geomorph.2015.06.026, 2015.
- Yager, E. M. and Schmeckle, M. W.: The influence of vegetation on turbulence and bed load transport, *J. Geophys. Res. Earth Surf.*, 118(3),
25 1585–1601, doi:10.1002/jgrf.20085, 2013.